Received July 28, 2015, accepted August 12, 2015, date of publication August 27, 2015, date of current version September 15, 2015.

Digital Object Identifier 10.1109/ACCESS.2015.2473661

Insights and Approaches for Low-Complexity 5G Small-Cell Base-Station Design for Indoor Dense Networks

DAVID MUIRHEAD[1], (Member, IEEE), MUHAMMAD ALI IMRAN[1], (Senior Member, IEEE), AND KAMRAN ARSHAD[2], (Member, IEEE)

[1]Institute for Communications Systems, University of Surrey, Guildford GU2 7XH, U.K.
[2]Department of Engineering Science Faculty of Engineering and Science, University of Greenwich at Medway Central Avenue, Chatham Maritime, Chatham ME4 4TB, U.K.

Corresponding author: D. Muirhead (d.muirhead@surrey.ac.uk)

ABSTRACT This paper investigates low-complexity approaches to small-cell base-station (SBS) design, suitable for future 5G millimeter-wave (mmWave) indoor deployments. Using large-scale antenna systems and high-bandwidth spectrum, such SBS can theoretically achieve the anticipated future data bandwidth demand of 10 000 fold in the next 20 years. We look to exploit small cell distances to simplify SBS design, particularly considering dense indoor installations. We compare theoretical results, based on a link budget analysis, with the system simulation of a densely deployed indoor network using appropriate mmWave channel propagation conditions. The frequency diverse bands of 28 and 72 GHz of the mmWave spectrum are assumed in the analysis. We investigate the performance of low-complexity approaches using a minimal number of antennas at the base station and the user equipment. Using the appropriate power consumption models and the state-of-the-art sub-component power usage, we determine the total power consumption and the energy efficiency of such systems. With mmWave being typified nonline-of-sight communication, we further investigate and propose the use of direct sequence spread spectrum as a means to overcome this, and discuss the use of multipath detection and combining as a suitable mechanism to maximize link reliability.

INDEX TERMS Air interface design, beamforming, densification, MIMO, mmWave, small cell, 5G.

I. INTRODUCTION

Wireless data traffic demands are anticipated to increase 1,000 fold by 2020 [1] and 10,000 fold by the year 2025 [2]. While approaches to maximize performance in the bands below 6GHz such as carrier aggregation, massive MIMO, coordinated multipoint (CoMP) and heterogeneous networks will improve things, these alone are believed to be insufficient [3]. Shrinking cell sizes through heterogeneity, greater spectral efficiency and, perhaps more significantly an increase in spectrum are seen as approaches to meet the needs of future networks [3], [4]. These come under the umbrella term of ''network densification'', comprising spatial densification and spectral aggregation [4]. Spatial densification is achieved by increasing the number of antennas per node and increasing the density of small base stations per m^2. Spectral aggregation relies on using fragments of spectrum from 500MHz to millimeter wave bands (30-300GHz) to form large bandwidths. However, this imposes significant transceiver design challenges. A better alternative solution is to use large contiguous spectrum found in the millimeter wave (mmWave) bands where large unused spectrum is available [3], [4]. Such bands can be used to provide a linear increase in capacity, proportional to the spectrum, to achieve very high peak and cell edge data rates. For example the 28 and 38GHz bands have 3-4GHz available and in the 70 and 80GHz E-band there is 10GHz available [3].

Traditionally for indoor communication, where the capacity demand is greatest, distributed antenna systems (DAS), microcells, relays and hotspots have been proposed. More recent advances in wireless networks have seen the introduction of the newly created wireless base station (BS) classification of 'small cells' or small cell base stations (SBS) being proposed. These include femtocells, picocells, microcells, and ultra-dense small cells where each sub-class is largely determined by the coverage area or cell radius it supports. In the case of the femtocell base

station (FBS) this will be in the order of tens of metres whereas picocell and microcell have an extended range from a few hundred metres to a few kilometers. Such SBSs along with WiFi access points are being proposed as a solution to data offloading to alleviate the congestion of today's cellular networks and improve the quality of service (QoS) for mobile end users [5].

The use of mmWave together with small cell densification using SBSs, are seen as enablers for future 5G systems to meet the anticipated capacity demand [2]. This is because design drivers for 5G include greater spectral efficiency (SE), peak data rates in the order of 10Gbps and low latency. In addition, very low power consumption of both access points and user terminals leading to greater energy efficiency (EE) and simple low cost design are required [6], [7].

Traditionally due to high propagation loss and lack of cost effective components mmWave frequencies have mostly been used for outdoor point to point backhaul links but not for cellular [8], [9]. While this perspective is changing, the high levels of attenuation loss for certain building materials (e.g. brick and concrete) may keep mmWave transmitted from outdoor base stations confined to outdoor structures [10]. Indoor coverage would in this case be provided by indoor SBS such as femtocells. The use of mmWave for indoor and personal area networks have long been considered attractive. However, the expense and power consumption of mmWave hardware has kept it from serious consideration as a cellular technology.

Recent advances in WiFi have seen the introduction of the 802.11ad standard using 60GHz mmWave frequencies to provide multi-gigabit per second throughput [11]. A feature of such networks is their low interference footprint which is attributable to excessive path loss beyond a certain distance. According to the Friss equation (1) (where P_r is the received power in unobstructed free space, P_t is the transmit power, G_t and G_r are the transmit and receive antenna gains and R is the distance between the transmitter and receiver in metres), distances of 10m, 60GHz suffers from 22dB more attenuation than 5GHz band and 30dB more than 2GHz band.

$$P_r = P_t + G_t + G_r + 20log_{10}\left(\frac{\lambda}{4\pi R}\right) \quad (1)$$

Therefore, communications in this range can be typified by extremely high throughput for very short distance (typically <10m) and by low interference to other surrounding networks due to high path loss. This provides greater spatial re-use, making it suitable for indoor cellular communications for SBSs such as femtocells in densely deployed networks.

Unlike outdoor mmWave communications, where large scale antenna systems (LSAS)/massive MIMO incorporating beamforming will be needed to overcome excessive path loss, indoor path loss looks more favorable. This suggests that SBSs equipped with single antennas may be capable of mmWave communications without the need for extensive power hungry antenna systems.

The contribution of this article is therefore to consider mmWave approaches to SBS design that exploit the short distance communication links that such devices will be deployed in. We consider the use of single omnidirectional antennas as well as multiple antenna beamforming. By performing link level simulation of a densely deployed apartment, using representative path models and channel conditions such as multipath dispersion, we show anticipated performance. Extensive Monte-Carlo simulations are provided to show performance for various levels of densification in such a deployment. We concentrate on the 28GHz and 72GHz bands because of their frequency separation as an appropriate mechanism to explore the performance of mmWave in these diverse bands. With low complexity and EE being drivers for 5G, we investigate the energy efficiency of such systems providing a Joules/bit metric based on performance and appropriate power consumption models. We further the investigation and consider the use of direct sequence spread spectrum (DS-SS) as a means of combating the effects of multipath and blocking in an indoor scenario.

This paper is organized as follows. Section II. Discusses design considerations based on relevant characteristics of mmWave for indoor communication drawing on recent state-of-the-art literature. Section III. provides insights into system performance of a densely deployed apartment block. Section IV. considers approaches to implementation of the communications transceiver and impacts on complexity and energy efficiency. The use of DS-SS for indoor mmWave is discussed in section V. Concluding remarks including key findings and directions for future research are given in Section VI.

II. INDOOR MILLIMETER WAVE - DESIGN CONSIDERATIONS

A. LINK BUDGET AND PATH LOSS

According to [10] the key factors that determine the downlink (DL) link budget of a millimeter wave system are the transmission power, the transmitter and receiver beamform gains and the path loss. By link budget analysis the authors show the anticipated data rates achievable over a 1km distance. The link budget assumes both antenna beamforming gain provided by multiple antennas at the transmitter and receiver to overcome significant path loss of between 121-129dB for mmWave using 28GHz and 72GHz. We further this analysis and consider small cell densification where the distance between the transmitter and receiver is expected to be small, in the order of 10s of meters. We compare both large and small cell link budget. Table 1. shows the achievable rates over a 1km and 10m distance, operating with a 28GHz and 72GHz carrier. For the 1km case high beamforming gains at the transmitter and receiver are assumed whereas only a single omnidirectional antenna is assumed in the 10m small cell.

The losses associated with feeder cable from the RF circuitry to the antenna in a conventional base station

TABLE 1. Large vs. small cell mmWave link budget showing reduced small cell path loss and and resultant significant small cell data rates for a reduced transmit power.

Large vs. Small Cell	Large 1	Large 2	Small 1	Small 2
Tx Power (dBm)	35	35	20	20
Beamforming Gain (dBi)	24	24	0	0
Carrier Frequency (GHz)	2.80E+10	7.20E+10	2.80E+10	7.20E+10
Distance (m)	1000	1000	10	10
Propagagion Loss (dB)	121.396889	129.60038	81.3968888	89.6003781
Other Losses	20	20	6	6
RxAntenna Gain (dBi)	15	15	0	0
Received Power (dBm)	-67.3968888	-75.600378	-67.396889	-75.600378
Bandwidth (GHz)	1.00E+09	1.00E+09	1.00E+09	1.00E+09
Thermal PSD (dBm/Hz)	-174	-174	-174	-174
Noise figure	10	10	10	10
Thermal Noise (dBm)	-7.40E+01	-7.40E+01	-7.40E+01	-7.40E+01
SNR (dB)	6.60311115	-1.6003781	6.60311115	-1.6003781
Implementation Loss (dB)	5	5	5	5
Data rate (bits/s)	1.29E+09	2.85E+08	1.29E+09	2.85E+08

can be significant. This together with other losses due to penetration, reflection and diffraction are accounted for as 20dB (equivalent to a 100 antenna element array gain) in [10] and are factored into our analysis shown in Table 1. For a SBS we ignore such feeder cable loss but factor in likely obstruction in the form of a 6dB drywall partition loss [10] as would be expected in an indoor office type deployment. The reduced distance in the small cell results in a much reduced propagation loss compared to the 1km case; 81.4dB for 10m compared to 121dB for a 1km cell for a carrier frequency of 28GHz. Significantly, the small cell omnidirectional system provides data rates that are actually the same as those over a 1km distance with a high beamforming gain.

RF measurement campaigns for indoor mmWave have been recently provided by Deng et al. [12]. Results for indoor propagation in the 73GHz band for both omnidirectional and directional antennas were provided. Omnidirectional co-polarized results show that the line of sight (LOS) path loss exponent is smaller than that of free space. This is attributed to ground bounces and constructive interference from reflections. These measurements were made for distances between the transmitter and receiver of 6 to 46m in a typical office environment. Other RF measurement campaigns in the mmWave such as [13] have shown that over short distances between 2 and 6m, in a Victorian office building, omnidirectional path loss is consistent with the Friss equation; however, significant multipath exists. The multipath is typified by a Rayleigh distribution despite line of sight, indicating the presences of strong reflection and scattering.

B. BLOCKING

Millimeter waves suffer severe penetration loss through solid materials e.g. 175dB loss through a 10cm thick concrete wall at 40GHz [10]. This leads to the conclusion that direct LOS communication will not always be possible. Fortunately measurement campaigns have shown that mmWave reflects well from the surface of blockages e.g. tinted glass and concrete [14]. This is important and Non-LOS (NLOS) paths created by reflections and refractions provide valuable energy which can be used to maintain a communication link.

C. MULTIPATH

It is widely known that multipath in wireless channels can lead to degraded QoS due to inter-symbol interference (ISI). In orthogonal frequency division multiplexing (OFDM) systems such as Long Term Evolution (LTE) 4G, this is completely eradicated since the coherence time of the channel is much larger than the delay spread of the multipath channel. The response of an OFDM sub-carrier can be considered as frequency flat and the need for equalization in the channel reception is not needed. It is important to consider the multipath delay profile in the mmWave band to determine the need for such equalization.

Measurements in [15] show delays spreads of 20ns for 60GHz in a single floor of a modern office building. Similarly, measurement results given in [16] show delays spreads of 18.08ns for 60GHz indoor modern office building when using an omnidirectional antenna. When directional antennas are used the delays spread reduces to 13.59, 4.7 and 1.05ns for wide, medium and narrow directional beam patterns. The delay spreads were based on multipaths appearing less than or equal to 50dB down from the main path. Other components were rejected. Indoor measurement at 17GHz [12], showed significant multipaths. Analysis of the fading suggested a Rayleigh distribution.

It is shown from measurements in [17] that delay spread is inversely proportional with the distance between the BS and mobile user which is explained by the observation that fewer dominant paths arrive due to the high path loss as the transmitter–receiver separation increases. The use of directional beamforming at the transmitter and receiver decreases the effect of delay spread since fewer multipaths will be captured in a focused narrow beam [14]. This infers we would expect significant multipath over short distances particularly when using omnidirectional antennas. Delay spread based on various indoor mmWave measurement and ray tracing campaigns are shown in Table 2.

TABLE 2. Indoor mmWave delay spread.

Freq	TX-RX Distance (m) /Area type	Delay Spread (ns)	Antenna Type
60GHz	9.2/ Modern office	20 [15]	Horn antenna
60GHz	13.51x7.81/ office	18.08 [16]	Omnidirectional
60GHz	13.51 x 7.81	1.05 [16]	Narrow beam
73GHz	6-46	35 [12]	Co-polarized (15° HPBW)
73GHz	6-46	20 [12]	Cross-polarized (15° HPBW)
17GHz	6/ Victorian office	Unspecified delay spread [13]	Omnidirectional

D. DOPPLER

The Doppler frequency of a wireless channel depends on the carrier frequency and mobility and in general increases linearly with the speed of the user equipment (UE) with respect to the base station. This would result in a Doppler frequency of 28Hz and 66Hz for moderate pedestrian UE speed of 1km/h at 28GHz and 72GHz respectively.

III. SYSTEM SIMULATION

Based on the design considerations outlined above, insights into system performance were performed my simulation.

A. SYSTEM MODEL

A densely deployed wireless network based on a 25 apartment block or a similar office block was used as the basis of our simulation model. Each apartment or office was modeled as 10m × 10m area forming a 50m × 50m total apartment area grid. A SBS equipped with a single omnidirectional antenna and then a DL beamformed uniform linear array (ULA) comprising 8 antennas, was considered. In both cases a single omnidirectional antenna was assumed at the UE. The UE uplink (UL) performance was simulated based on the DL transmission method. SBSs were randomly dropped on the grid for a particular block loading (10, 25, 50, 75 and 100%) where 100% corresponds to an active SBS in each apartment.

For each SBS, a single served UE was dropped randomly within the apartment with respect to this. The channel link margin was modeled as per Table 1. ('Small1' and 'Small2') where the path loss model is based on the Friss model with appropriate losses. This is pessimistic considering the reduced path loss exponent findings for indoor in [10]. A 6dB loss was assumed for interior drywall partition in the apartment block based on [10]. Each SBS transmitted a pseudo randomly generated data stream, using a quadrature phase shift keyed (QPSK) constellation. An example of a 50% loaded apartment is shown in Fig. 1.

B. SIMULATIONS

To determine the performance of the mmWave the following cases were considered:

1) Single omnidirectional antenna case with 10, 25, 50, 75 and 100% block loadings, carrier frequency $f_c = 28$GHz.
2) Single omnidirectional antenna case with 10, 25, 50, 75 and 100% block loadings, carrier frequency $f_c = 72$GHz.
3) 8×1 MISO DL beamformer case with 10, 25, 50, 75 and 100% apartment loadings, carrier frequency $f_c = 28$GHz.
4) 8×1 MISO DL beamformer case with 10, 25, 50, 75 and 100% apartment loadings, carrier frequency $f_c = 72$GHz.

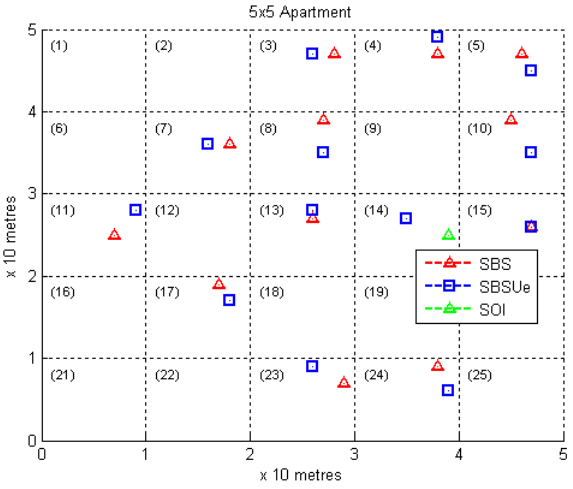

FIGURE 1. Simulated dense deployment showing a 50% loaded apartment block.

For each loading case, a Monte Carlo simulation consisting of 3000 simulation iterations was performed. For each iteration, SBSs were randomly dropped on the grid and a SBS of interest (SOI) was randomly selected. The performance (SINR and BER) of the SOI's UE's UL was computed according to placement of other SBSs in the grid and grid loading. The parameters used in the simulations are listed Table 3.

TABLE 3. Parameters used.

Parameter	Value
Bandwidth	625 MHz
Modulation	QPSK
Symbol Rate	500 MSPS
BS Tx Antenna Type	Omnidirectional, 8x ULA
Carrier Frequency	28GHz, 72GHz
UE Rx Antenna Type	Omnidirectional
Channel Model	2-tap Rayleigh: [0ns, (0dB), 20ns (-10dB)]
Doppler Frequency	28Hz @28GHz 66Hz @72GHz
Tx Power	20dBm
Channel Estimation	Ideal
Tx-Rx filter	0.25 root raised cosine
Rx Equalizer	None

In such a system, the performance of the receiver system at the UE will be affected by the delay spread and whether symbol equalization is used or not. As discussed in section II, using a single omnidirectional antenna at the receiver is more likely to provide significant multipath capture. We therefore model the channel with a two-tap Rayleigh fading channel using a 0dB main LOS path and a second path NLOS path delayed by 20ns and −10dB with respect to the main path. This is based on the interpolating the results shown in Table 2. Doppler frequencies of 28Hz and 66Hz are used corresponding to a maximum UE mobility of 1km/h for the 28 and 72GHz carrier frequencies. The UE receiver in the

SOI was modeled as a simple QPSK matched filter without equalization.

C. RESULTS AND DISCUSSION

BER measurements are shown in Fig. 2. This illustrates the uncoded and unequalized performance of the receiving UE served by the SOI. The performance improvement due to the increased SINR of the beamformed system is apparent.

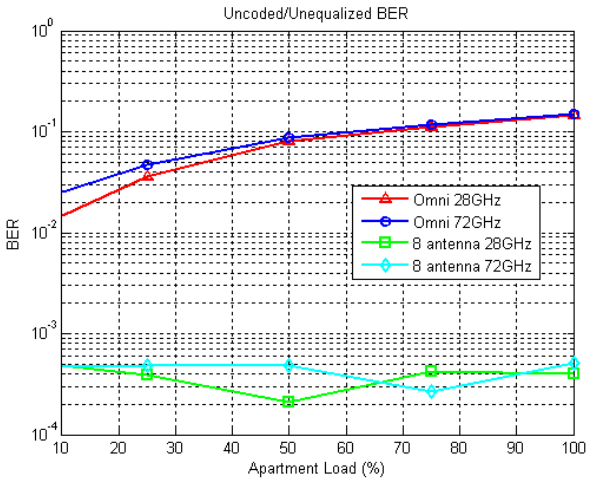

FIGURE 2. Uncoded and unequalized BER results highlighting the relative performance due to the increased SINR provided by the beamformer.

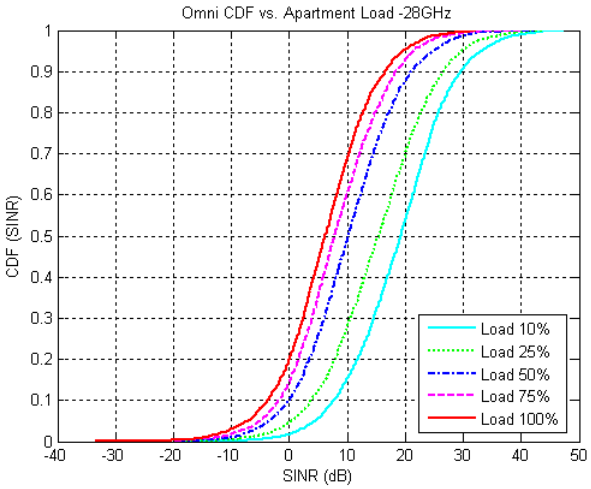

FIGURE 3. SINR results for a carrier frequency $f_c = 28$GHz. A 14dB reduction in SINR is given as the apartment load is increased from 10 to 100%.

The results shown in Fig. 3-Fig. 8 generally illustrate the effect of propagation as a function of frequency of operation for the two carrier frequencies used. The impact of the apartment loading is evident on the performance and shows a 14dB reduction in SINR at 28GHz as the loading is increased from 10% to 100%. For the 72GHz case a similar trend is observed; however, the performance is less affected by load and an average of 9dB reduction in SINR is given. This shows the isolation due to the difference in carrier frequency i.e. as the frequency is increased so are the path losses of

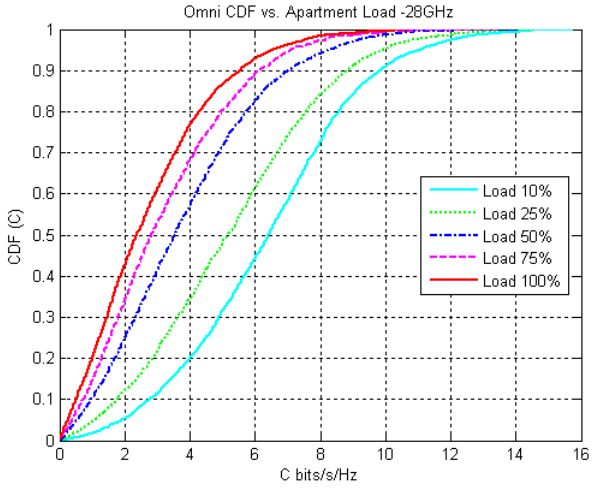

FIGURE 4. Spectral efficiency for a carrier frequency $f_c = 28$GHz using an omnidirectional antenna at both transmitter and receiver.

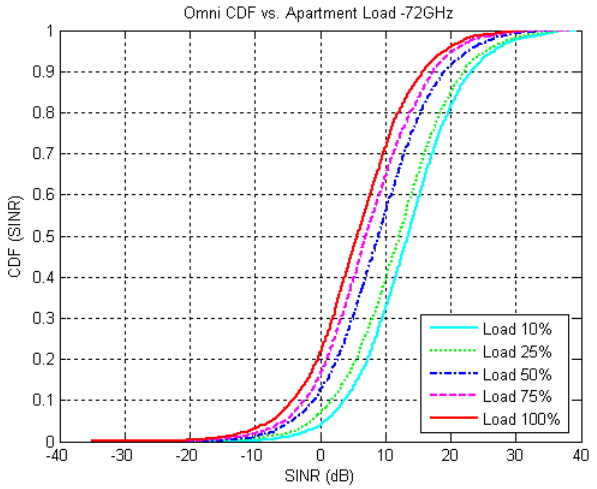

FIGURE 5. SINR results for a carrier frequency $f_c = 72$GHz. A 9dB reduction in SINR is given as the apartment load is increased from 10 to 100%.

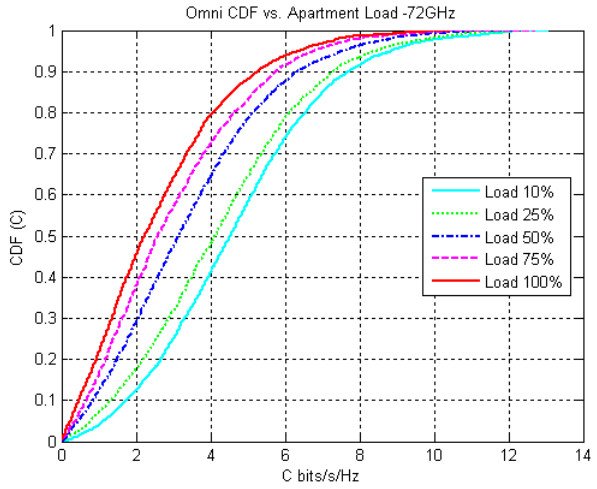

FIGURE 6. Spectral efficiency for a carrier frequency $f_c = 72$GHz using an omnidirectional antenna at both transmitter and receiver.

the interferers. This is clearly exemplified considering the results of the DL beamforming system shown in Fig. 7. The results give insights into the performance improvement by not

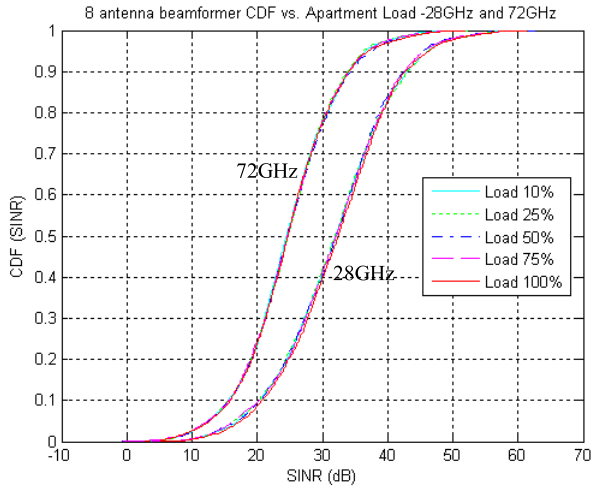

FIGURE 7. SINR results for 28GHz and 72GHz – 8 Antenna beamformed DL. Beamforming gain sufficient to keep SINR based on signal level and receiver noise floor. Apartment loading has negligible effect.

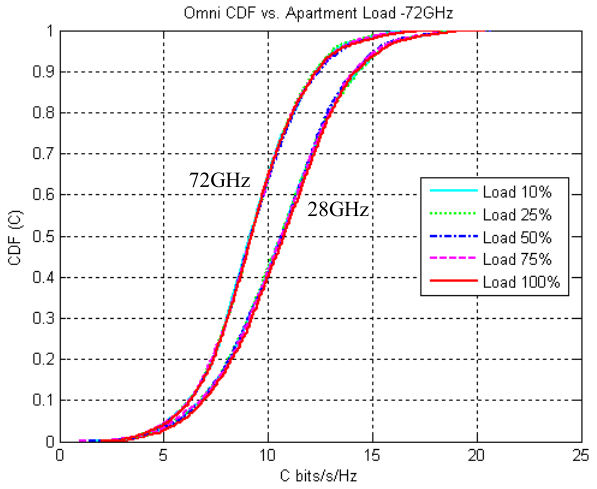

FIGURE 8. Spectral efficiency for 28GHz and 72GHz – 8 Antenna beamformed DL, showing how the spectral efficiency is affected by the frequency of operation.

only the beamforming gain but the isolation of surrounding co-channel SBSs. Here the additional beamforming gain ensures that the SINR is dominated by the wanted signal and the receiver noise floor and not by the surrounding SBSs, which are attenuated sufficiently to appear below the receiver noise floor. This shows the immunity of the 5G system to interference in such a deployment. The spectral efficiency of the omnidirectional 10% loaded system is shown to give an average 6.3 and 4.3 bits/s/Hz for 28GHz and 72GHz carrier frequencies respectively (see Fig. 4 and & Fig. 6). Using Shannon's capacity equation these should theoretically achieve 3.15Gbits/s and 2.15Gbits/s respectively assuming a 500MHz channel bandwidth. The use of beamforming to overcome eroded link margin is a logical design decision. However, cellular systems may need to transmit omnidirectional signals where 360° coverage maybe required; for instance in a residential dwelling. The omnidirectional results are therefore of significance for this use case. A spectral efficiency of 8.3 and 10.6 bits/s/Hz was provided for the 8-antenna beamformed system (see Fig. 8). Assuming a 500MHz bandwidth, data rates of 4.15 and 5.3 Gbits/s would be possible for the 72GHz and 28GHz system respectively.

IV. BEAMFORMING COMPLEXITY AND ENERGY EFFICIENCY

Low power consumption of both access points (SBS) and UEs together with simple low cost design are seen as drivers for 5G [6], [7]. Using our simulated results we explore the power consumption and energy efficiency of possible transceiver architectures for 5G namely omnidirectional, digital beamforming or RF beamforming as the DL transmission mode.

A. BEAMFORMING ARCHITECTURES

Full digital beamforming, where a transceiver stage is required per antenna, is seen as impractical because of the excessive power requirements the analogue to digital conversion (ADC) and digital to analogue converter (DAC) stages of each transceiver incur at mmWave frequencies [18]. In addition, as the sampling rate of such ADCs increases so does the inaccuracy of the conversion due to aperture jitter [19]. This has led to alternative approaches being considered such as designing systems that would traditionally require 8-12 bits of dynamic range to use less than this e.g. 4 bits such that the overall ADC power is reduced. These systems are suited to applications requiring smaller dynamic range such as LOS communications employing small constellations [20]. Whether a communications can be constrained to such levels of quantization is subject to debate. Alternatively the authors in [20] consider using a number of low speed, high precision ADCs operating in parallel to synthesize a high-speed, high precision ADC. This approach is subject mismatches between sub-component ADCs which require compensation.

The main approach to overcome the ADC/DAC problem is to employ beamforming at the RF level rather than at the digital baseband. In this case the many antenna elements are served by only a single ADC/DAC per sector [18].

Digital beamforming is illustrated in Fig. 9 and shows the requirement for an RF transceiver comprising up and down conversion together with DAC and ADC devices. Each transceiver is required for every antenna element in the system. The approach is common in current 3G and 4G systems employing MIMO technologies but is thought to be unsuitable to satisfy the low power requirements of 5G. The alternative RF beamforming approach is illustrated in Fig. 10. Here a single transceiver drives an antenna array. Channel weights associated with the intended user, or group of users are applied at the RF with simple phase changing components.

The choice of implementation is biased by the power usage argument but there are advantages and disadvantages of both approaches. These are outlined in Table 4.

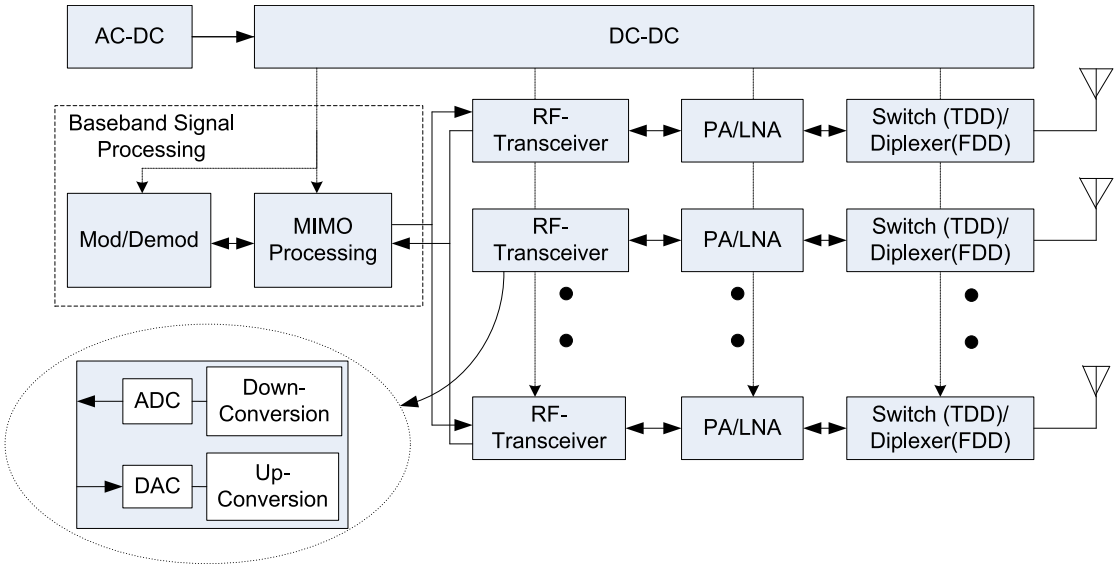

FIGURE 9. Digital beamforming modem.

TABLE 4. Advantages and disadvantages of beamforming approach.

Type	Advantages	Disadvantages
RF Beamforming	Single or few transceiver chains meaning lower power consumption due to limited nos. of ADC/DAC for many antennas.	Less flexible than digital beamformer. Implies users are separated in time thus puts constraints on implementation. Difficult to get channel estimates if at RF.
Digital Beamforming	Null steering/zero forcing possible since channel responses known at baseband. Best performance/higher degree of freedom.	Significant power consumption and cost due to high speed ADC/DAC required in each transceiver.

B. POWER AND ENERGY EFFICIENCY

To determine the energy efficiency we consider the energy consumption ratio (ECR) this gives us the energy per delivered information bit.

$$ECR = \frac{E}{K} = \frac{PT}{K} = \frac{P}{D}\ [J/bit] \tag{2}$$

where E is the energy required to deliver K bits of information over time T, and $D = K/T$ is the data rate in bits per second. This provides us with the energy consumption in Joules consumed for transportation of one information bit.

Use of the total power (P) consumed by the SBS, and not simply the transmit power, is an important consideration to make. As previous research has shown [21]–[23] the use of realistic power consumption models (PCMs) determining the overall expended base station power are essential to predict the energy efficiency of a system. Static PCMs provide a detailed breakdown of the main components of a SBS and assume full load with maximum transmit power. Unlike a larger BS, cooling power and feeder losses are omitted in the power model of our analysis. Static PCMs can be used to assess the overall power consumption required for a given multiple antenna embodiment. The PCM given in (3) provides us with the total power consumed (P'_{Tot}) considering the processing (RF and Baseband) requirements of the DL beamforming solution.

$$P'_{Tot} = \left[N_{PA} \left(\frac{P_{PA}/\mu_{PA}}{N_{PA}} \right) + P_{TRX} + (N_{PA} - 1) \cdot \frac{P_{TRX}}{2} + P_{SP} + \gamma P_{SP} \right] \tag{3}$$

When considering the losses due to the supply and conversion of electricity to the system, the total power can be determined as (4). Here DC-DC conversion loss (P_{DCLoss}) and power supply loss P_{PSLoss} are given as proportional to the respective sub-systems they feed shown in Fig. 9 & (3). The total consumed power is therefore defined as:

$$P_{Tot} = P'_{Tot} + P'_{Tot} \cdot P_{DCLoss} + \left(P'_{Tot} \cdot P_{DCLoss} \right) \cdot P_{PSLoss} \tag{4}$$

The parameters applicable to (3) and (4) are shown in Table 5.

High power mmWave systems that are currently used for backhaul applications over long distances comprise components such as power amplifiers (PAs), transceivers, low noise amplifiers (LNAs), mixers and antennas that are physically too big in size and consume too much power to be applicable to cellular communications. However with the technologies for 60GHz WLAN (IEEE 802.11ad) and Wireless HD (IEEE 802.15.3c) being standardized, suitable integrated circuit (IC) based transceivers are becoming available [10].

Provision of suitable values for our PCM was accomplished by a review of recent advances in mmWave technology [24] and performing a search of commercially available mmWave components [25], [26]. The use of a 12-bit ADC

TABLE 5. PCM parameters.

Parameter	Description
N_{PA}	Number of power amplifiers
P_{PA}	Transmit Power (W)
μ_{PA}	PA efficiency
P_{TRX}	RF transceiver power – single radio, considering both transmit and receive functions (W)
P_{SP}	Signal processing power – single radio (W)
γ	Signal processing overhead power factor (%)
P'_{Tot}	Total power consumed for antenna beamforming sub-system system.
P_{DCLoss}	DC-DC loss conversion loss (%)
P_{PSLoss}	Power supply loss (%)
P_{Tot}	Total power for antenna beamforming scheme (W) including power supply and conversion loss.

operating at 4GSPs (8 × oversampling for 500MHz bandwidth) [25] and a 16-bit DAC operating at 2.8GSPs [26] were considered. The ADC and DAC components comprise RF down and up-conversion respectively. A mains-DC conversion efficiency of 8% and a DC-DC conversion efficiency of 10% were assumed. Based on the mmWave CMOS power amplifiers given in [24] a PA efficiency (μ_{PA}) of 5% was assumed for a 20dBm transmit power P_{PA}. The PAs in [24] are intended for use at 60GHz but provided a realistic basis for mmWave PA efficiency. It was assumed that the baseband signal processing power (P_{SP}) was zero for the architectures considered. In a practical system this will not be the case, particularly for the digital beamforming solution. However, low order modulation schemes e.g. binary phase shift keying (BPSK) or QPSK, with a simple matched filter demodulators without equalization are assumed for both systems.

TABLE 6. Power and energy efficiency.

System	P_{Tot} (W)	ECR (J/bit)
Omni (28GHz)	6.38	$2.03\text{x}10^{-9}$
Omni (72GHz)		$2.97\text{x}10^{-9}$
Digital beamformer (28GHz)	29.23	$5.73\text{x}10^{-9}$
Digital beamformer (72GHz)		$6.50\text{x}10^{-9}$
RF beamformer (28GHz)	6.38	$1.25\text{x}10^{-9}$
RF beamformer (72GHz)		$1.42\text{x}10^{-9}$

The total power and equivalent ECRs for the system operating with a 500MHz bandwidth are provided in Table 6. Using the derived ECR values in Table 6. the relative energy efficiency of each system with respect to the digital beamformer was determined. Here the energy reduction gain (ERG) was used as the basis of the calculation and can be found as:

$$ERG = \frac{ECR_1 - ECR_2}{ECR_1} \cdot 100\% \quad (5)$$

where ECR_1 and ECR_2 correspond to the energy consumption ratio of two different systems. The results show a 78% energy reduction of the RF beamforming solution for both 28GHz and 72GHz. Significantly the omnidirectional antenna case shows a 64% and 54% reduction in energy expenditure for 28GHz and 72GHz respectively.

V. SPREAD SPECTRUM FOR INDOOR mmWAVE

A. DRAWBACKS OF LSAS FOR INDOOR

Many researchers are optimistic that the beamforming gains provided by LSAS, such as path loss compensation and lower multipath delay spread capture, will facilitate simple receiver architectures through low complexity waveforms [10] e.g. QPSK. In this case, such receivers would comprise simple matched filters and would not require expensive and complex signal processing in the form of equalization. However, there are issues with this for which alternative approaches should be considered, particularly for short indoor distances. As an example the amount of channel estimation required to formulate appropriate beamforming weights, required for either RF or digital beamforming, will be significant and will impact complexity and power. For frequency division duplex systems (FDD) this will be particularly acute. Furthermore, NLOS communication and channel blocking effects are a cause for concern. As this article as highlighted the use of mmWave, particularly for short distances such as indoor scenarios, is subject to multipath dispersion which can be caused by reflection from blockages or the physical properties of the building concerned. In this case NLOS communication may be the only possible means to overcome such effects i.e. the gain from beamforming may still be insufficient if the blockage causes a significantly large attenuation of the transmitted signal. The reliability of such links may be challenging when relying on beamforming alone [27]. In such cases, and because the multipath may appear outside of the antenna beam, re-acquisition, identification and further antenna steering or beamforming may be required to find any available multipath energy. To minimize these effects it is therefore desirable to make use of all available multipath energy, including instantaneous multipath from blocking, and use it in a constructive way to improve the performance of the system.

B. DIRECT SEQUENCE-SPREAD SPECTRUM

It is well known that in direct sequence-spread spectrum (DS-SS) information is transmitted using a wider bandwidth than necessary. Here data bits from the source $b(t)$ are multiplied by a code signal $c(t)$ at a faster rate known as the chip rate. The process is referred to as spreading and the amount of spreading is determined by the spreading factor (SF). At the receiver of such a system, the use of a Rake Receiver effectively performs the equalization task by combining the received signal with multiple, time delayed versions of it (the multipaths) separated by multiples of the chip period (T_c). This allows the components of the original

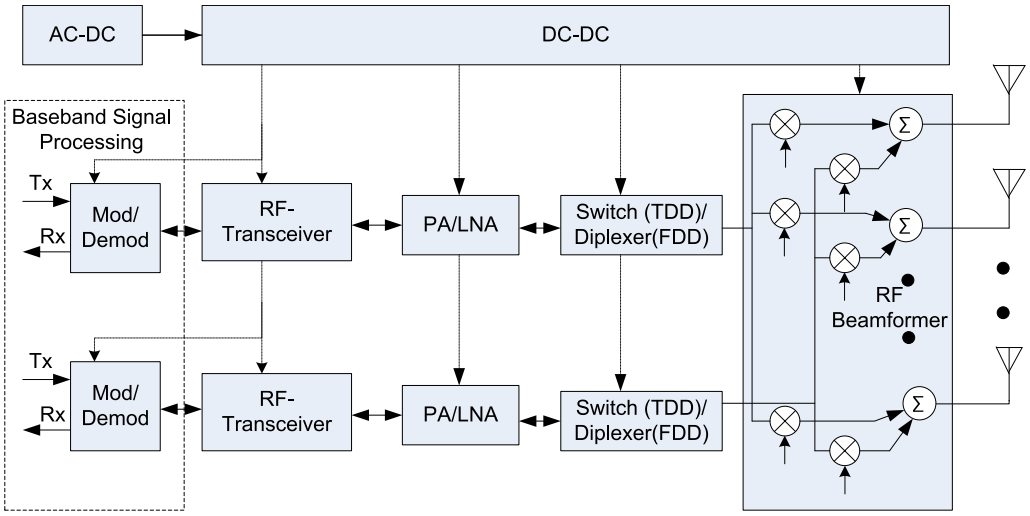

FIGURE 10. RF beamforming model.

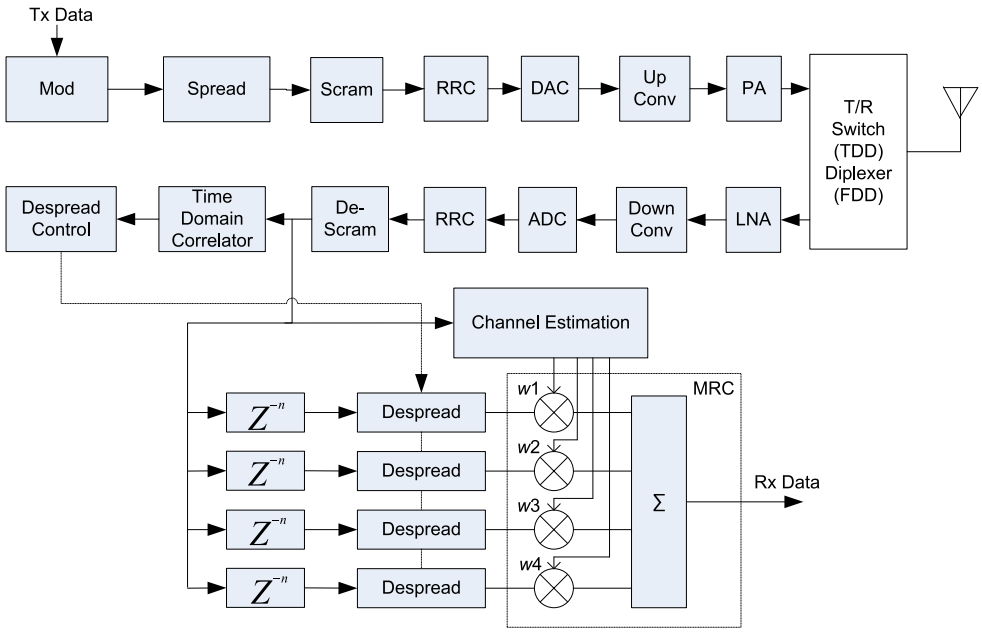

FIGURE 11. DS-SS Transceiver.

signal to be recovered with the time delays removed. Maximum ratio combining (MRC) of the delayed signals yields an optimal output which has a maximum possible signal to noise ratio given the input signals [28]. As in other equalizers e.g. Viterbi the performance can be calculated from the performance of the MRC of the each of the channel multipaths [28]. However, for DS-SS greater performance is expected because the increased bandwidth of the spread signal allows the receiver to resolve multipath energy which would otherwise appear combined in a single channel tap [28]. In this sense the spreading mechanism gives us the ability to find available energy and use it to our advantage. This therefore increases the effective diversity order and all available energy can be identified and used to increase the signal to noise ratio (SNR) of the signal.

To summarize, in most receiver design multipath creates inter symbol interference that requires potentially complex equalization techniques. In the case of a spread spectrum system such multipath components can be used in a constructive way to improve the performance of the system by detecting and combining the main and delayed multipath components in a Rake Receiver. In this case multipath actually provides additional improvements in the system performance.

1) PROPOSED SYSTEM

We propose a simplified air interface for an indoor communications system operating in the mmWave frequencies based on a DS-SS. The proposed architecture for the transceiver is shown in Fig. 11 and comprises spreading and scrambling in the transmit path. Scrambling is used to identify users in the

uplink and minimize interference in the DL. Corresponding descrambling and despreading is performed in the receive path. Identification of multipath elements in a transmission can be performed using the time domain correlator, implemented as a code matched filter (CMF), who's taps are equivalent to a local and known spreading and scrambling code sequence multiplied by known pilot symbols. Assuming a single antenna system the channel estimation complexity is determined by the number of expected multipaths. In a small cell this would be expected to be low and potentially less than the number of antenna elements in a beamforming system. A Rake Receiver and an MRC are used to combine the multipath components identified by the correlator.

The motivation and advantages of such a system are as follows:

I. Spreading and scrambling allows the identification of delay and multipath components by correlating the transmitted signal with a local copy of the spreading/scrambling code.
II. Unlike other systems the multipaths in DS-SS can be used to perform constructive combining at the receiver with a Rake receiver. This therefore provides additional gain in the form of diversity gain and provides resistance to blocking and multipath dispersion.
III. Large bandwidth exists in the mmWave bands to facilitate the additional spectrum needed by the spreading process.
IV. The spreading and scrambling processes can be considered as low complexity. Arguably the most complex part is the time domain correlator but since its complexity is driven by delay spread this will be minimal in an indoor deployment where the distance will be small.
V. Low peak to average power ratio (PAPR) compared to more complex modulation envelopes or multi-carrier systems meaning more efficient use of power amplifiers.

The disadvantage with such a scheme is the effective waste of bandwidth due to the spreading process i.e. for every symbol transmitted SF x system bandwidth is needed. Additionally, due to the higher effective signal bandwidth the ADC and DAC components will be required to clock yet higher meaning greater power consumption. In general it is preferred that the ADC has large spurious free dynamic range (SFDR) meaning large order ADC devices e.g. 12-bit. However, to reduce power consumption the use of smaller dynamic range ADCs could be suitable for short distances as discussed in [20]. Unlike OFDM systems, DS-SS is a single carrier system meaning it has a lower peak-to-average power ratio (PAPR). Using low order modulation schemes such as BPSK or QPSK would allow the use of ADCs with a smaller dynamic range.

The link budget of a small cell based on DS-SS is shown in Table 7. The use of a moderate amount of DL beamforming, using a 4×1 MISO configuration is assumed. No beamforming is assumed at the receiver. Spreading factors of SF=4 and SF=8 are used as examples. Particularly for the SF=4, the achievable data rates are comparable with those in Table 1 but due to the spreading and multipath detection process should provide better mitigation to blocking and the effects of multipath.

TABLE 7. DS-SS link budget–spreading is used to overcome path loss and facilitate multipath detection and constructive combining.

Small Cell Link Budget	Case1	Case2	Case3	Case4
Tx Power (dBm)	20	20	20	20
Beamforming Gain (dBi)	6	6	6	6
Carrier Frequency (GHz)	2.80E+10	7.20E+10	2.80E+10	7.20E+10
Distance (m)	10	10	10	10
Propagagion Loss (dB)	81.3968888	89.60037815	81.3968888	89.60037815
Spreading Factor	4	4	8	8
Other Losses	6	6	6	6
Received Power (dBm)	-61.3968888	-69.6003781	-61.3968888	-69.6003781
Bandwidth (GHz)	2.00E+09	2.00E+09	2.00E+09	2.00E+09
Thermal PSD (dBm/Hz)	-174	-174	-174	-174
Noise figure	10	10	10	10
Thermal Noise (dBm)	-7.10E+01	-7.10E+01	-7.10E+01	-7.10E+01
SNR (dB)	9.5928112	1.389321894	9.5928112	1.389321894
Implementation Loss (dB)	3	3	3	3
Data rate (bits/s)	1.24E+09	3.79E+08	6.19E+08	1.89E+08

VI. CONCLUSIONS AND FUTURE THEMES

This paper has provided important insights into the design and performance of small cells in dense indoor networks. Using findings from recent measurement campaigns, we have discussed the fundamental design considerations and link budget analysis and used these to implement and simulate a densely deployed indoor network. Anticipated spectral efficiency of omnidirectional and beamformed systems has been provided. We have shown that the use of single antenna systems provides significant achievable data rates as well as indicating more spectrally efficient performance for a moderate number of antennas operating in a DL beamforming configuration. Using appropriate power consumption models and energy metrics, the energy efficiency of these approaches has been provided illustrating the motivation to use RF beamforming over a full digital beamformed system. Significantly the use of omnidirectional antennas has been shown to provide substantial data rates in an energy efficient manner compared to a digital beamformed system.

We further extended the analysis to consider the use of spread spectrum as a means to overcome NLOS and multipath propagation. Future research themes for small cells should consider this approach and look to address the needs higher oversampling rates traded off against lower dynamic range as may be possible in a small cell indoor deployment.

With the likelihood that there will exist an abundance of available transmitted RF energy in dense 5G networks, coupled with the use of LSAS at base station and UE devices, the possibility of RF energy harvesting should be considered as a future area of research.

REFERENCES

[1] B. Raaf *et al.*, "Vision for beyond 4G broadband radio systems," in *Proc. IEEE 22nd Int. Symp. Pers. Indoor Mobile Radio Commun. (PIMRC)*, Sep. 2011, pp. 2369–2373.

[2] M. Cudak, *et al.*, "Moving towards mmwave-based beyond-4G (B-4G) technology," in *Proc. IEEE 77th Veh. Tech. Conf. (VTC Spring)*, vol. 2, no. 5, pp. 1–5, Jun. 2013.
[3] A. Ghosh *et al.*, "Millimeter-wave enhanced local area systems: A high-data-rate approach for future wireless networks," *IEEE J. Sel. Areas Commun.*, vol. 32, no. 6, pp. 1152–1163, Jun. 2014.
[4] N. Bhushan *et al.*, "Network densification: The dominant theme for wireless evolution into 5G," *IEEE Commun. Mag.*, vol. 52, no. 2, pp. 82–89, Feb. 2014.
[5] L. Liu, X. Chen, M. Bennis, G. Xue, and Z. Han, "A distributed ADMM approach for mobile data offloading in software defined network," in *Proc. Wireless Commun. Netw. Conf. (WCNC)*, Mar. 2015, pp. 1748–1752.
[6] C. Rowell, S. Han, Z. Xu, and I. C. Lin, "Green RF technologies for 5G networks," in *Proc. IEEE Int. Wireless Symp. (IWS)*, Mar. 2014, pp. 1–4.
[7] P. Mogensen *et al.*, "5G small cell optimized radio design," in *Proc. IEEE Globecom Workshops (GC Wkshps)*, Dec. 2013, pp. 111–116.
[8] W. Roh *et al.*, "Millimeter-wave beamforming as an enabling technology for 5G cellular communications: Theoretical feasibility and prototype results," *IEEE Commun. Mag.*, vol. 52, no. 2, pp. 106–113, Feb. 2014.
[9] S. Rajagopal, S. Abu-Surra, and M. Malmirchegini, "Channel feasibility for outdoor non-line-of-sight mmWave mobile communication," in *Proc. IEEE Vehicular Technol. Conf. (VTC Fall)*, Sep. 2012, pp. 1–6.
[10] Z. Pi and F. Khan, "An introduction to millimeter-wave mobile broadband systems," *IEEE Commun. Mag.*, vol. 49, no. 6, pp. 101–107, Jun. 2011.
[11] T. Nitsche, C. Cordeiro, A. B. Flores, E. W. Knightly, E. Perahia, and J. C. Widmer, "IEEE 802.11ad: Directional 60 GHz communication for multi-gigabit-per-second Wi-Fi [Invited Paper]," *IEEE Commun. Mag.*, vol. 52, no. 12, pp. 132–141, Dec. 2014.
[12] S. Deng, C. J. Slezak, G. R. MacCartney, Jr., and T. S. Rappaport, "Small wavelengths—Big potential: Millimeter wave propagation measurements for 5G," *Microw. J.*, Nov. 2014.
[13] H. Radi, M. Fiacco, M. A. N. Parks, and S. R. Saunders, "Simultaneous indoor propagation measurements at 17 and 60 GHz for wireless local area networks," in *Proc. 48th IEEE Vehicular Technol. Conf. (VTC)*, vol. 1. May 1998, pp. 510–514.
[14] T. S. Rappaport *et al.*, "Millimeter wave mobile communications for 5G cellular: It will work!" *IEEE Access*, vol. 1, pp. 335–349, 2013.
[15] C. R. Anderson and T. S. Rappaport, "In-building wideband partition loss measurements at 2.5 and 60 GHz," *IEEE Trans. Wireless Commun.*, vol. 3, no. 3, pp. 922–928, May 2004.
[16] T. Manabe, Y. Miura, and T. Ihara, "Effects of antenna directivity and polarization on indoor multipath propagation characteristics at 60 GHz," *IEEE J. Sel. Areas Commun.*, vol. 14, no. 3, pp. 441–448, Apr. 1996.
[17] T. S. Rappaport, F. Gutierrez, E. Ben-Dor, J. N. Murdock, Y. Qiao, and J. I. Tamir, "Broadband millimeter-wave propagation measurements and models using adaptive-beam antennas for outdoor urban cellular communications," *IEEE Trans. Antennas Propag.*, vol. 61, no. 4, pp. 1850–1859, Apr. 2013.
[18] F. W. Vook, A. Ghosh, and T. A. Thomas, "MIMO and beamforming solutions for 5G technology," in *Proc. IEEE MTT-S Int. Microw. Symp. (IMS)*, Jun. 2014, pp. 1–4.
[19] R. H. Walden, "Analog-to-digital converter survey and analysis," *IEEE J. Sel. Areas Commun.*, vol. 17, no. 4, pp. 539–550, Apr. 1999.
[20] J. Singh, S. Ponnuru, and U. Madhow, "Multi-gigabit communication: The ADC bottleneck," in *Proc. IEEE Int. Conf. Ultra-Wideband (ICUWB)*, Sep. 2009, pp. 22–27.
[21] *Energy Efficiency Analysis of the Reference Systems, Areas of Improvement and Target Breakdown, Version 2.0*, EARTH Project Deliverable D2.3, Jan. 2012.
[22] O. Arnold, F. Richter, G. Fettweis, and O. Blume, "Power consumption modeling of different base station types in heterogeneous cellular networks," in *Proc. Future Netw. Mobile Summit*, Jun. 2010, pp. 1–8.
[23] F. Heliot, M. A. Imran, and R. Tafazolli, "On the energy efficiency gain of MIMO communication under various power consumption models," in *Proc. Future Netw. Mobile Summit (FutureNetw)*, Jun. 2011, pp. 1–9.
[24] F. Shirinfar, M. Nariman, T. Sowlati, M. Rofougaran, R. Rofougaran, and S. Pamarti, "A fully integrated 22.6 dBm mm-wave PA in 40 nm CMOS," in *Proc. IEEE Radio Freq. Integr. Circuits Symp. (RFIC)*, Jun. 2013, pp. 279–282.
[25] *ADC12J400 12-Bit 4 GSPS ADC With Integrated DDC*. [Online]. Available: http://www.ti.com/lit/ds/symlink/adc12j4000.pdf, accessed Jun. 2015.
[26] *DAC39J84 Quad-Channel, 16-bit, 2.8GSPS, Digital-to-Analog Converter with 12.5 Gbps JESD204B Interface*. [Online]. Available: http://www.ti.com/lit/ds/symlink/dac39j84.pdf, accessed Jun. 2015.
[27] D. Da Silva *et al.*, "Tight integration of new 5G air interface and LTE to fulfill 5G requirements," in *Proc. IEEE 81st Vehicular Technol. Conf. (VTC Spring)*, May 2015, pp. 1–5.
[28] S. R. Saunders, "Equalisers," in *Antennas and Propagation for Wireless Communication Systems*, 1st ed. Chichester, U.K.: Wiley, 1999, pp. 358–361.

DAVID MUIRHEAD (M'12) received the B.Eng. (Hons.) degree in electronics engineering from the University of Central England, Birmingham, in 1996, and the M.Sc. (Hons.) degree in mobile and personal radio communications from Lancaster University, in 2002. He is currently pursuing the Ph.D. degree with the Institute for Communications Systems, University of Surrey.

He was with Lucent Technologies and Picochip Ltd., where he was involved in ASIC and software systems for 3G and WIMAX small cell base stations. He is with Honeywell as a Technical Manager of the satellite communications systems team responsible for the implementation of next-generation satellite communications systems and modems.

MUHAMMAD ALI IMRAN (M'03–SM'12) received the B.Sc. (Hons.) degree in electrical engineering from the University of Engineering and Technology Lahore, Pakistan, in 1999, and the M.Sc. (Hons.) and Ph.D. degrees from Imperial College London, U.K., in 2002 and 2007, respectively. He received the Award of Excellence in recognition of his academic achievements from the President of Pakistan.

He has been actively involved in European Commission funded research projects ROCKET and EARTH, Mobile VCE funded project on fundamental capacity limits, EPSRC funded project India-U.K. ATC, and QNRF funded QSON project. He is currently a Reader with the Institute for Communications Systems, University of Surrey, U.K. He is the Principal Investigator of EPSRC funded REDUCE project. He is the work area leader for the 5G Innovation Centre's New Physical Layer. His main research interests include the analysis and modeling of the physical layer, optimization for the energy efficient wireless communication networks, and the evaluation of the fundamental capacity limits of wireless networks.

KAMRAN ARSHAD (M'15) received the B.Eng. and M.Sc. (Hons.) degrees in electrical engineering in 2000 and 2003, respectively, and the Ph.D. degree from Middlesex University London, in 2007.

He has been associated with the University of Greenwich, U.K., as a Senior Lecturer and the Program Director of M.Sc. Wireless Mobile Communications Systems Engineering since 2012. He is pursuing research interests in Physical layer layer, cognitive radio, 5G, Long Term Evolution (LTE)/LTE-advanced, and cognitive machine-to-machine communications. He has authored over 80 technical peer-reviewed papers in journals and international conferences, and received three best paper awards. He is a Senior Fellow of the U.K. Higher Education Academy.